A LINEARIZED FREE-SURFACE RANS METHOD FOR SHIP MANEUVERING

MARINE 2019

PAOLO GEREMIA*, KEVIN J. MAKI† AND PAVLOS ALEXIAS†*

* ENGYS S.R.L.
Strada per Vienna, 9
34151 Trieste, Italy
Email: p.geremia@engys.com - Web page: http://www.engys.com

† University of Michigan
Ann Arbor, Michigan, USA
Email: kjmaki@umich.edu - Web page: http://cshl.engin.umich.edu/

†* ENGYS Ltd
Studio 20 - Royal Victoria Patriotic Building, John Archer Way,
London SW18 3SX, United Kingdom
Email: p.alexias@engys.com - Web page: http://www.engys.com

Key words: CFD, free-surface, maneuvering, PMM, self-propulsion

Abstract. Proper prediction of ship maneuvering – together with powering and seakeeping – is considered essential these days to help naval architects design optimal ship hulls. In this context, traditional finite-volume Computational Fluid Dynamics (CFD) methods offer a well-proven simulation platform to realize such predictions with a high degree of certainty. In this work, a novel transient CFD method based on a linearized free-surface RANS solver is presented to assess maneuvering actions of both captive and free-running ship performance on a series of selected test cases. The performance of the proposed solver is considerably better in terms of solution speed than other traditional CFD methods employed for this type of analysis, especially when applied to transient solutions requiring long simulation times.

1 INTRODUCTION

CFD solvers employed in the study of ship hull hydrodynamics are usually based on either Volume-Of-Fluid (VOF) [1] or level-set methods [2], both implemented as part of the Reynolds Averaged Navier Stokes (RANS) equations in a finite-volume framework. Albeit these methods have proven to deliver highly accurate predictions for hull resistance and other important performance parameters, they often require very long computational times which are incompatible with the time available at the early stages of the design process. During the ship design process, different design candidates must be evaluated by the designers and, ideally, fast turnaround times are required to quickly screen multiple layouts to find an optimal solution for the hull.

In order to overcome the high computational costs associated to traditional VOF and level-set methods, a new RANS based Linearized Free-Surface (LFS) solver with viscous effects was successfully implemented and employed to perform fast hull-form optimization using a steady-state formulation [3], which allowed for faster predictions of hull resistance and other parameters without compromising the overall accuracy of the results.

In this paper, the original steady-state LFS solver described in [3] has been extended to enable time-dependent solutions using an unsteady RANS (uRANS) formulation. The new unsteady solver has also been modified to incorporate a full 6 Degrees-of-Freedom (DoF) rigid body motion framework in order to simulate a variety of hull motions, including calm-water resistance, seakeeping, maneuvering and self-propulsion.

The use of the uRANS approach is of significant importance to accurately predict both the pressure and viscous forces acting on the hull, including the interaction with the propeller and the rudder components. In this context, the application of the LFS solver allows for a more efficient solution in terms of computational time, hence allowing the designer to investigate the effects of multiple hull motions in shorter times.

The current implementation of the new unsteady LFS solver is limited for now to in-plane motions only (namely: surge, sway and yaw) due to the nature of the rigid-body 6DoF library employed. Therefore, all model tests and validations presented herein are focused on Planar Motion Mechanism (PMM) and free-running 3DoF maneuvering tests, assuming negligible roll and pitch angles at low running speeds.

2 DESCRIPTION OF FLOW SOLVER

The proposed uRANS LFS flow solver is based on the linearized unsteady Neumann-Kelvin ship wave boundary-value problem. The ship generated wave is assumed to be of small wave amplitude and steepness, and the fully-nonlinear free-surface boundary condition can be satisfied in linearized form on the calm-water plane. This allows for a double-body discretization to be used together with a single-phase flow solver.

In the present work, the unsteady kinematic condition is coupled to the unsteady uRANS equations via the dynamic free-surface condition that is applied to the free-surface boundary of the domain. The mathematical details and extensive validation of the formulation can be found in [6, 9].

One improvement, unique to this solver, is the way in which the 3DoF dynamic mesh motion and the Multiple Reference Frame (MRF) are applied. In this case, the entire domain translates and rotates with the geometry while the reference frame remains earth-fixed [4]. This improves the accuracy when solving the non-linear equations, the ability to simulate wave patterns and the solver's robustness.

The 3DoF motion capabilities make this model applicable to a wide range of problems, including the free-fall of a body that impacts the air-water interface, the seakeeping response of a surface vessel or submarine, or the maneuvering response of a ship.

3 CAPTIVE TEST CASES

The first application considered in this paper is a series of PMM captive tests performed on the KRISO Container Ship (KCS) model [5]. The characteristics of the hull are summarized in Table 1.

2

Table 1: KCS Geometry and conditions for PMM tests

Scale	52.667
Lpp [m]	4.3671
Bwl [m]	0.6114
T [m]	0.2051
U [m/s]	1.701
Fn [-]	0.26

The maneuvering simulation tests are performed in even keel conditions with dynamic sinkage and trim suppressed to mimic the results obtained in the towing tank experiments when using the PMM system. In the uRANS method employed for all the captive tests described in this work, the two equations $k\text{-}\omega$ *SST* turbulence model was used due to its accurate prediction of pressure forces when applied to ship hydrodynamics.

To assess the convergence of the rigid-body motion library applied to the LFS solver, a preliminary mesh convergence study was carried out in preparation for the subsequent captive test simulations performed [6].

3.1 Static Drift

The first test performed as part of this study was a static drift maneuver of the KCS model with a yaw amplitude $\xi_6 = 5deg$ simulation, travelling at a constant speed at $Fn = 0.26$ in calm-water conditions, with a 2.5s ramp applied in which the body is accelerated until it reaches the target nominal speed.

The main objective of this task was to carry out a grid convergence study and determine a convergence criterion for both the sway force and the yaw moment calculated on the hull on a coarse, medium and fine grid with 321K, 843K and 2.8M cells, respectively. The mesh layout and the resulting free-surface elevation for the fine mesh case are shown in Figure 1.
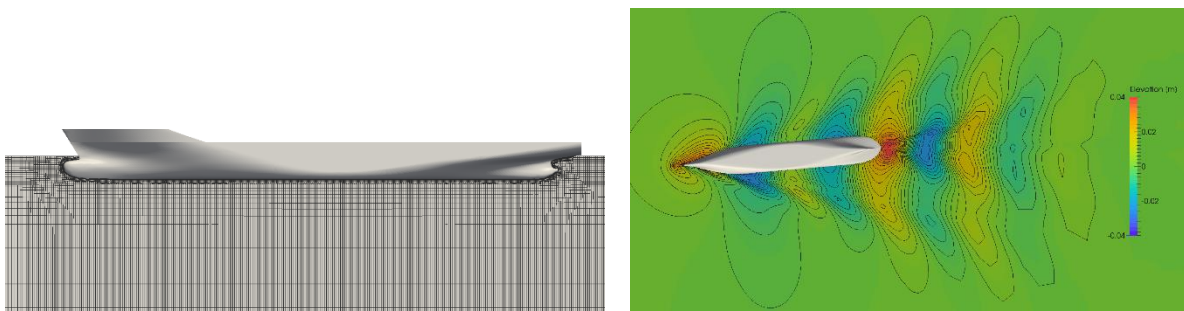

Figure 1: Static Drift: fine mesh overview (left) and free-surface elevation (right)

To check the convergence of the solver against the grid size, the sway force and yaw moment output responses were considered. Assuming h_i as the reference size of the i-th grid, where h_1 is the fine mesh reference cell size, the Richardson extrapolated exact solution ϕ_0 was defined starting from the ϕ_1, ϕ_2 and ϕ_3 measured responses for the fine, medium and coarse grids respectively, according to the following formula:

3

$$\phi_0 = \phi_1 + \frac{\phi_1 - \phi_2}{r^p - 1} \tag{1}$$

where p is the order of the interpolation defined as follows:

$$p = \frac{ln[(\phi_3 - \phi_2)/(\phi_2 - \phi_1)]}{ln(r)} \tag{2}$$

And $r = h_{i+1}/h_i$ is the constant ratio of refinement between the grids. The extrapolated solution ϕ_0 as well the mesh extrapolation curves are shown in Figure 2 for both the sway force and the yaw moment.
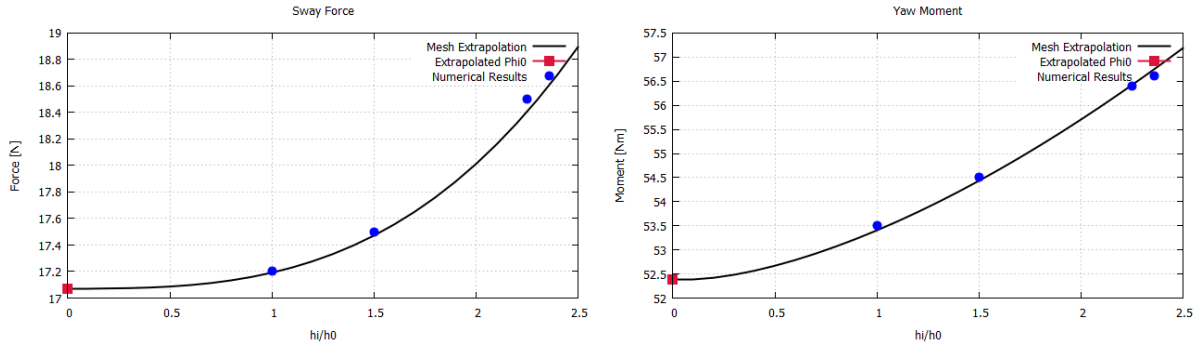

Figure 2: Mesh extrapolation: sway force (left) and yaw moment (right)

It can be noticed that a monotone convergence is achieved for both the forces considered in Figure 2. The same can be also seen if the Grid Convergence Index (GCI) is defined as follows:

$$GCI = 1.25 \frac{|\phi_{i+1} - \phi_i|}{\phi_i} \frac{1}{r^p - 1} \tag{3}$$

In fact, an asymptotic range of convergence is obtained for both sway force and yaw moment, as follows:

$$\left(\frac{GCI_2}{r^p GCI_1}\right)_{Surge\ Force} = 0.984 \approx 1 \tag{4}$$

$$\left(\frac{GCI_2}{r^p GCI_1}\right)_{Yaw\ Moment} = 0.980 \approx 1$$

The same grid and numerical setup employed for the static drift run was thus used for running two additional captive tests, namely: a pure sway and a pure yaw PMM maneuvers, as detailed in the following sections.

3.2 Pure Sway

A pure sway maneuver was carried out with a sway amplitude of $\xi2 = 0.127$m and a PMM period of 13.33s. For this purpose, a total of 34CPU hours (defined as number of processors multiplied by the clock time for each PMM period) was required.

The results in terms of sway force and yaw moment were compared against the experimental measurements provided by FORCE Technology and made available for the SIMMAN 2014
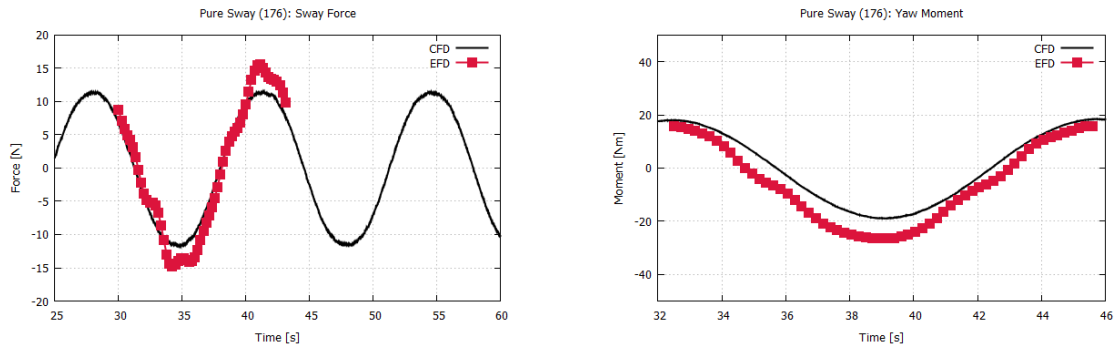
4

workshop [7].

Figure 3: Pure sway forces: CFD vs. experiments

Figure 3 shows the comparison between CFD and experiments for the hydrodynamic forces as a function of time. It can be clearly noticed that the new uRANS LFS solver predicts correctly both the amplitude and the frequency of the time series compared to the experiments, with just a few asymmetries in the forces noticed in the experiments which cannot be reproduced in the CFD simulation.

3.3 Pure Yaw

The pure yaw forced motion was performed using a sway amplitude of $\xi_2 = 0.297$m, a yaw amplitude $\xi_6 = 4.7$deg and a PMM period of 13.33s. The time series of the forces predicted with the uRANS LFS solver are compared to the experiments in Figure 4.
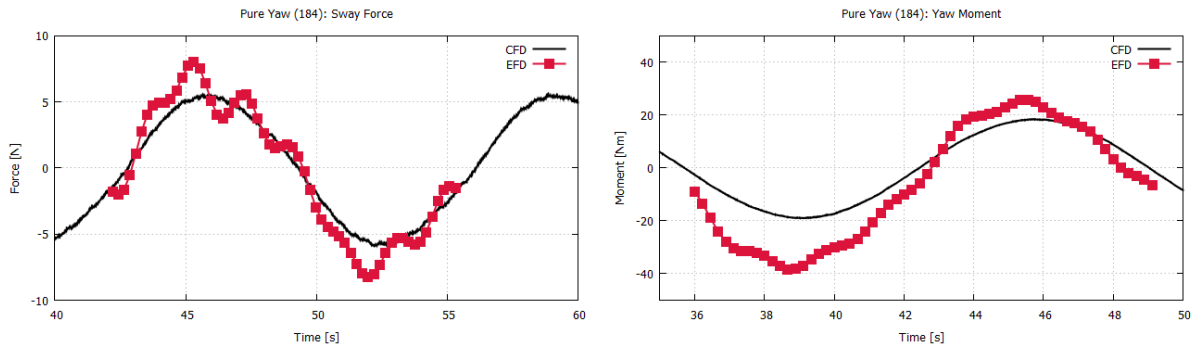

Figure 4: Pure yaw forces: CFD vs. experiments

In this case, high-frequency components in the experiments not visible in the CFD results for the sway force can be identified. The yaw moment instead, shows that the maximum value of the moment is correctly predicted, whereas the minimum is underpredicted and this again is due to an asymmetry in the experimental results. For the pure yaw case the total CPU time per PMM period was set to 34.8 CPU hours, which was quite in line with the turnaround times required for the pure sway case.

4 SELF-PROPULSION TESTS

The new uRANS LFS solver was also employed on a series of free-running tests, including

5

self-propulsion, turning circle and zig-zag maneuvers. In the work detailed here though, only the results of the self-propulsion tests are presented.

The test case considered for the self-propulsion simulation is the KCS hull form according to the Gothenburg 2010 Case 2.3a workshop specifications [8]. The aim of this test was to evaluate the accuracy of the uRANS LFS solver to predict maneuvering operations, which require the inclusion of the propulsion system modelling. Typically, this type of simulations entails considerable computational efforts when employing traditional fully non-linear uRANS methods, such as VOF based solvers. The KCS model test conditions are outlined in Table 2.

Table 2: KCS Geometry and conditions for the self-propulsion test

Scale	31.600
Lpp [m]	7.2785
Bwl [m]	1.019
T [m]	0.3418
U [m/s]	2.196
Fn [-]	0.26
S/L^2	0.1781

The self-propulsion test was carried out at the ship point in calm-water conditions to reproduce the test setup. A fixed rotational speed was applied to the propeller in order to determine the towing force measured during the experiments and defined as $(R_t\text{-}T)$, where R_t is the hull resistance force and T is the propeller thrust.

In order to assess the accuracy and the performance of the uRANS LFS solver, the results obtained with this solver were compared to results obtained using a VOF type solver. In both cases, the same rigid-body motion self-propulsion framework was employed, assuming an initial 10s time ramp to accelerate both the body motion and the propeller speed to match the nominal target conditions. Also in both cases, the *k-ω SST* turbulence model was applied and a transient sliding mesh approach was employed to model the propeller rotation using Arbitrary Mesh Interface (AMI). No rudder was considered in the models.

4.1 Model Setup

Two computational grids were created, one for the VOF case and another one for the uRANS LFS solver case. The background block mesh employed to create both grids used the same anisotropic refinements near the free-surface to ensure a correct prediction of the wave-making resistance, as well as high-aspect ratio cells in the far field to reduce the total cell count. Near-wall layers with an overall y+ of 60 were defined on the hull body walls, and the same surface and volume refinement levels were applied to both grids to ensure a fair and consistent comparison between both methods.

The total cell count achieved using this approach was 3.44M for the VOF grid and 2.7M cells for uRANS LFS grid, with the latter mesh having less cells only because the air domain is ignored in favor of the first-order free-surface boundary condition applied at the free-surface. The resulting grids are both shown in Figure 5.
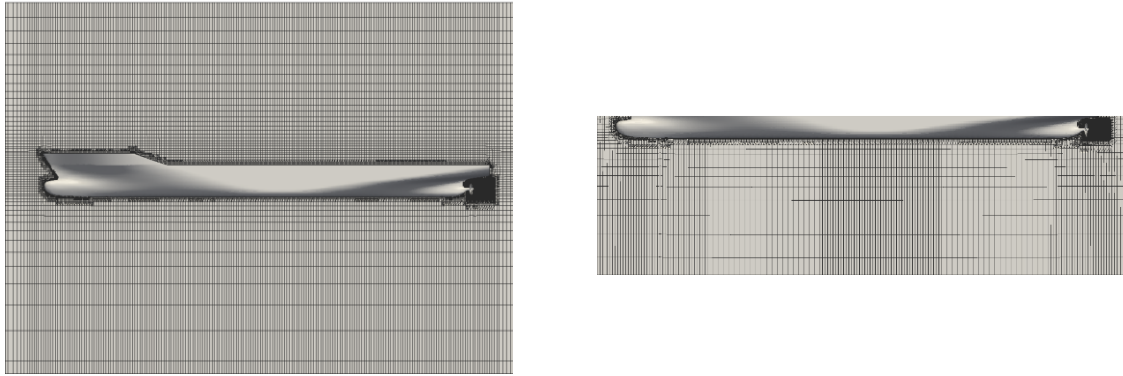
6

Figure 5: Computational grid for VOF (left) and uRANS LFS (right) solver cases

In terms of solver settings, the same discretization schemes were employed in both cases for time (first-order Euler) and advection (second-order). In the VOF model, 3 outer correctors without relaxation were employed, whereas only 2 outer correctors were required for the uRANS LFS solver. All the degrees of freedom were enforced in both solvers.

Furthermore, a maximum CFL of 10 was set for the initial phase of the VOF simulation to reach converged conditions. Similarly, in the uRANS LFS solver case, the initial phase was completed using a maximum CFL of 100. In both simulations, a finer time step was employed after completing the initial phase of the runs to model a 1deg-span of the propeller revolution to correctly predict the thrust and torque forces.

4.2 Self-propulsion Results

The free-surface elevation field and the vorticity near the propeller are shown in Figure 6 for the uRANS LFS solver. This solution was achieved in 295 CPU hours, as opposed to the 4,980 CPU hours it took to reach the same level of convergence using the VOF solver.
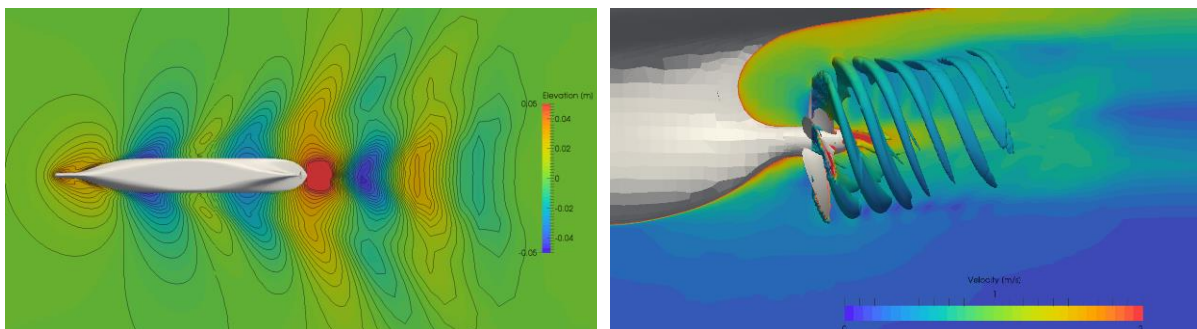

Figure 6: Free-surface elevation (left) and vorticity field (right) for the LFS case

Table 3 compares the experimental data (EFD) and simulation results for the forces obtained using the VOF and uRANS LFS solvers.

7

Table 3: Self-propulsion simulation results

	CFD				EFD			
Solver Type	Ct	Rt(SP)-T [N]	Kt	Kq	Ct	Rt(SP)-T	Kt	Kq
VOF	0.003891	28.7	0.170	0.0311	-1.9%	-5.1%	-0.1%	8.1%
LFS	0.004005	33.4	0.164	0.0318	1.0%	10.4%	-3.8%	10.5%

The results obtained with the uRANS LFS solver show a good agreement with the experiments for both the propeller and hull forces. It can be observed that the uRANS LFS solver tends to underpredict the propeller thrust and overpredict the torque forces with respect to the VOF solver and experimental measurements. This is expected due to the approximate nature of the LFS method against the fully non-linear uRANS equations used in the VOF solver.

Figure 7 shows the axial velocity contours downstream of propeller plane at $x/Lpp=0.9911$ from the experiments, VOF and uRANS LFS solver simulations. Although the CFD results presented are instantaneous values of the axial velocity, it can be seen that the wake behavior is consistent between the VOF and LFS cases, and that both simulations are in a good agreement with the averaged results available from the experiments.
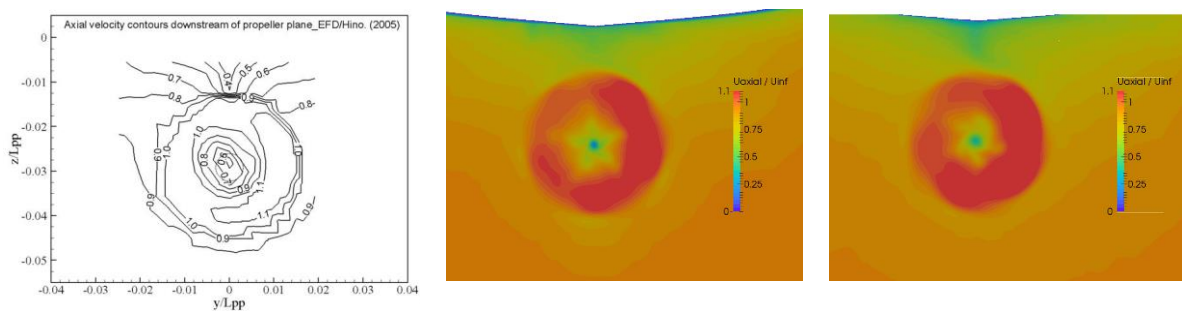

Figure 7: Axial velocity contours at $x/Lpp=0.9911$: EFD (left), VOF (center) and LFS (right)

Finally, Figure 8 shows the velocity components downstream of the propeller plane for both simulation cases. The results show good agreement between the VOF and uRANS LFS solvers in terms of axial and transverse velocities. However, the comparison with the experiments are clearly better for axial velocity than transverse velocities in both cases.
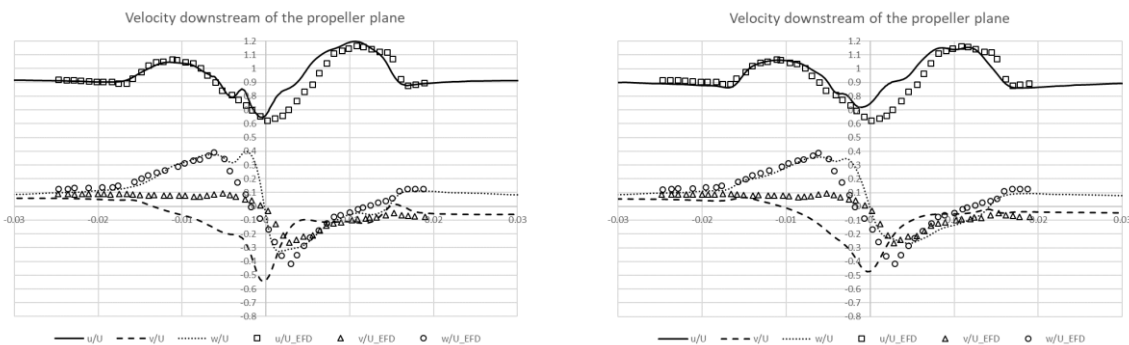

Figure 8: Velocity at $x/Lpp=0.9911$ and $z/Lpp=-0.03$: CFD vs. EFD for the VOF (left) and LFS (right) solvers

8

5 CONCLUSIONS

In this work, an innovative unsteady CFD solver based on the Linearized Free-Surface (LFS) approach has been presented as a novel approach to simulate ship hull maneuvering. The proposed LFS solver was validated against a series of well-known test-cases. The results achieved with the new solver for both captive and free-running tests showed that it provides a viable and more cost-effective alternative than traditional VOF methods without compromising in accuracy. The LFS solver can also run with CFL numbers 10 times higher than the equivalent VOF methods to deliver faster solutions for the correct prediction of ship behavior in the early stages of the design process. Further work is being carried out at present to validate the linearized free-surface solver framework for more complex free-running maneuvers, such as turning circle and zig-zag tests. Results of these additional test will be presented by the same authors in future works.

REFERENCES

[1] W. Xu, G. Filip, and K.J. Maki "A Method for the Prediciton of Extreme Ship Responses using Design-Event Theory and Computational Fluid Dynamics", *Journal of Ship Research*, under review.

[2] A. Di Mascio, R. Broglia, and R. Muscari "On the Application of the Single-Phase Level-Set Method to Naval Hydrodynamic Flows", *Computers and Fluids,* **36**(2007), 868-886.

[3] W. J. Rosemurgy, D. O. Edmund, K. J. Maki, and R. F. Beck "A Method for Resistance Prediction in the Design Environment", *11th International Conference on Fast Sea Transportation*, 2011.

[4] Maki, K. and Piro, D. "Whipping response of a box barge in oblique seas". *28th International Workshop on Water Waves and Floating Bodies,* 2013.

[5] W.J. Kim, S.H. Van, D.H. Kim. "Measurements of Flows around modern commercial ship models". In: *Experiments in Fluids*, **31**(2001), 567-578.

[6] M. O. Woolliscroft, "A Linearized Free-Surface Method for Prediction of Unsteady Ship Maneuvering", *PhD Thesis*, University of Michigan, USA, 2015.

[7] J.F. Otzen, C.D. Simonsen editors, *Proceedings SIMMAN 2014 Workshop*, Copenhagen, Denmark, 2014.

[8] L. Larsson, F. Stern, M. Visonneau editors, *Gothenburg 2010 A Workshop on Numerical Ship Hydrodynamics - Proceedings, Volume II*, Gothenburg, Sweden, 2010.

[9] Woolliscroft, M. O., and K. J. Maki. "A fast-running CFD formulation for unsteady ship maneuvering performance prediction." *Ocean Engineering* **117**(2016), 154-162.

9